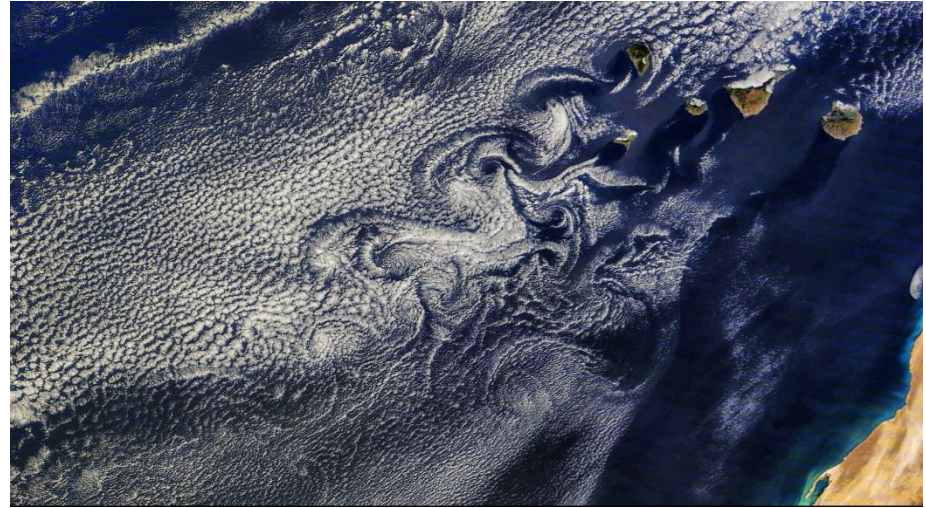
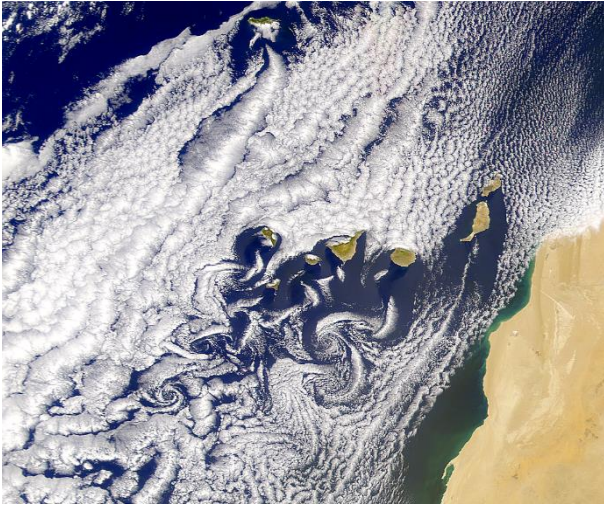


Representation of orographic effects in models

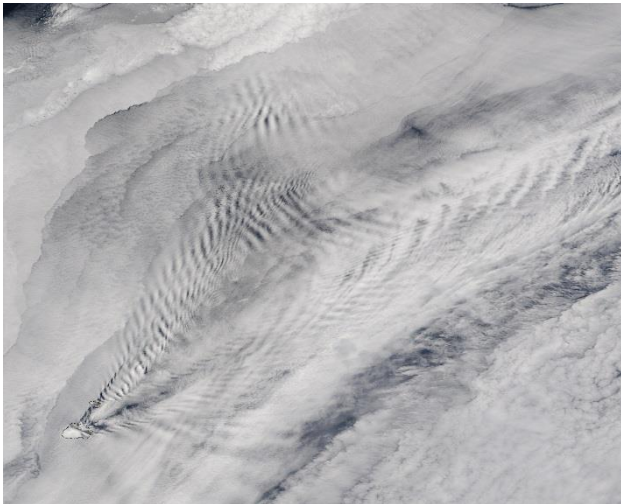
Irina Sandu & Anton Beljaars

Effects of orography on the flow

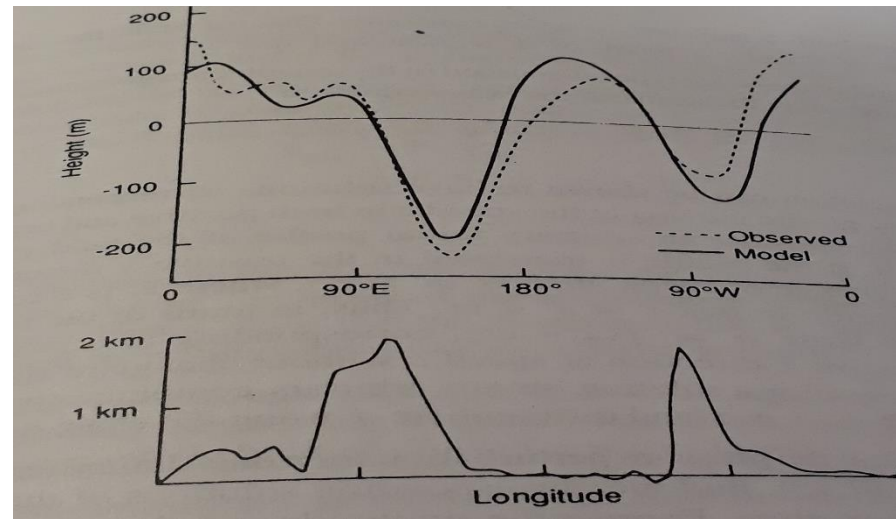
Wakes & von Karman vortices



Lee wave clouds



Winter mean longitudinal distribution of geopotential heights at 500hPa



Charney and Elianssen (1949)

Outline

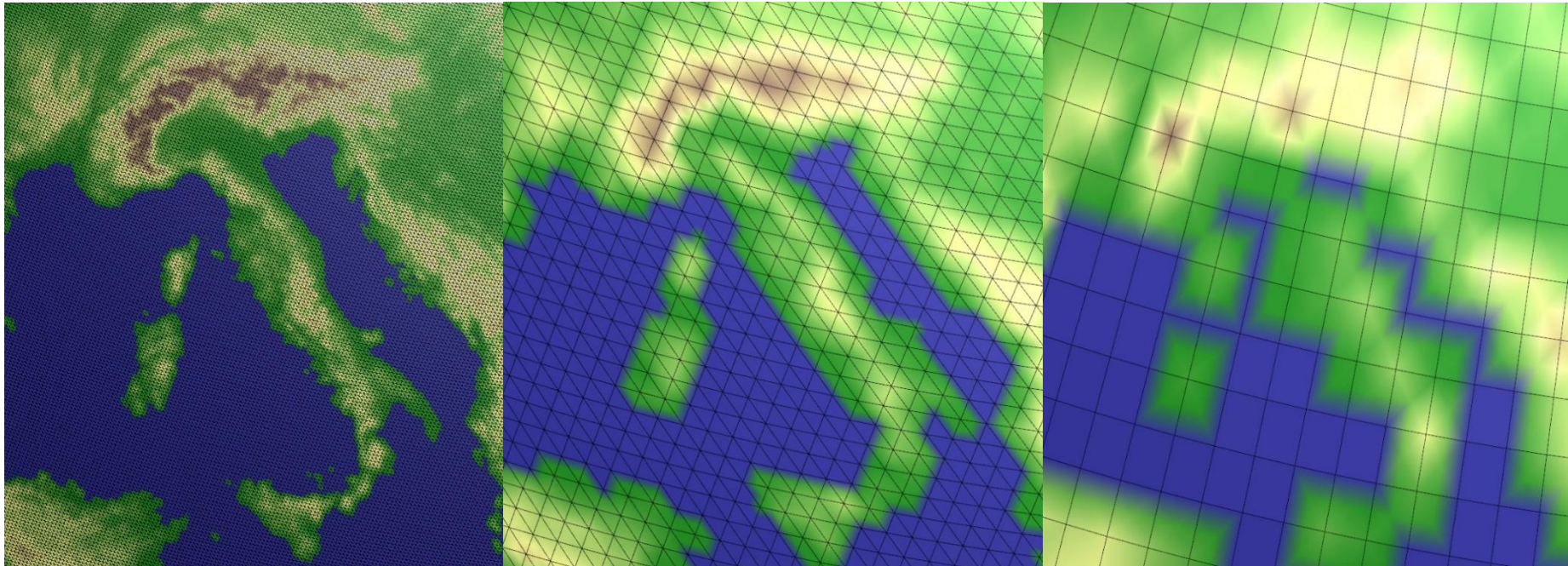
- Resolved and subgrid orography
- Orographic drag schemes
- Uncertainties in the representation of orographic drag and impacts on the large-scale circulation

Why do we need to parametrize orographic effects?

Orography at 9 km resolution

Orography at 50 km resolution

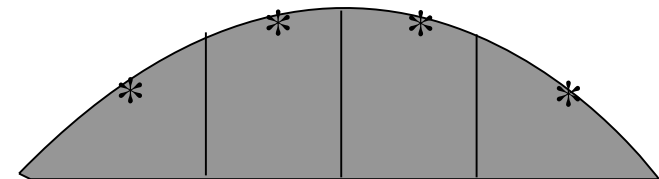
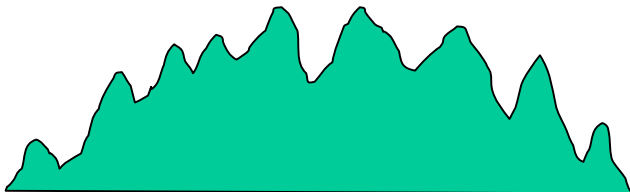
Orography at 125 km resolution



Global NWP models



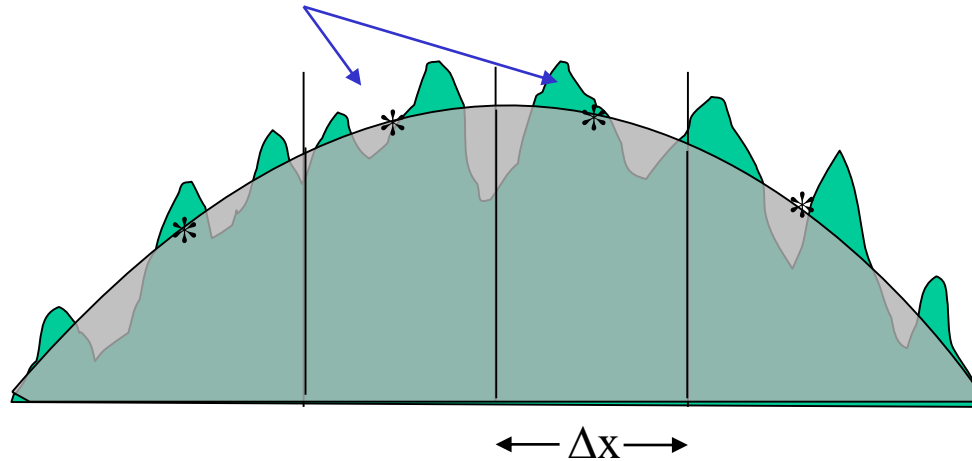
Global climate models



Models cannot directly resolve detailed surface features,
and more generally processes at subgrid scale

Resolved & subgrid orography

Use h to derive the mean (resolved) topographic height at each gridpoint



h : topographic height above sea level
(from global 1km data set)

$$\vec{\tau} = \vec{\tau}^{res} + \vec{\tau}^{phy}$$

$$\vec{\tau}^{res} = p_s \vec{\nabla} h = \text{resolved orographic stress}$$

$$\vec{\tau}^{phy} = \vec{\tau}^{pbl} + \vec{\tau}^{sgo} = \text{unresolved (subgrid) stress}$$

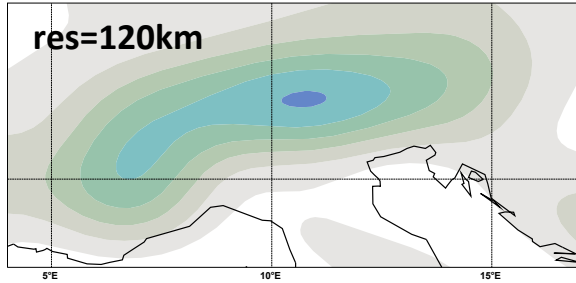
Resolution sensitivity of resolved/subgrid fields

mean orography
/ land sea mask

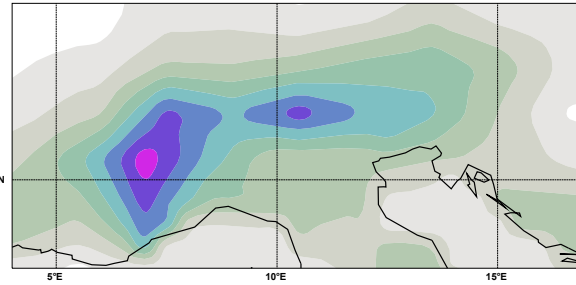
standard deviation (μ)

slope (σ)

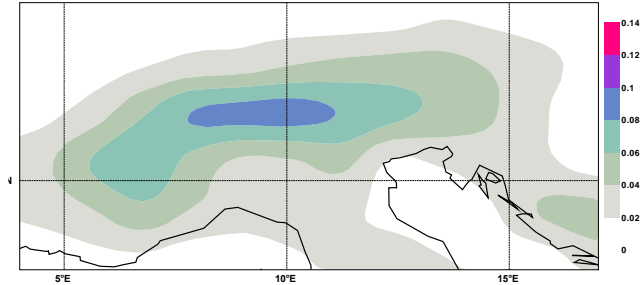
ERA40 mean orography/land sea mask



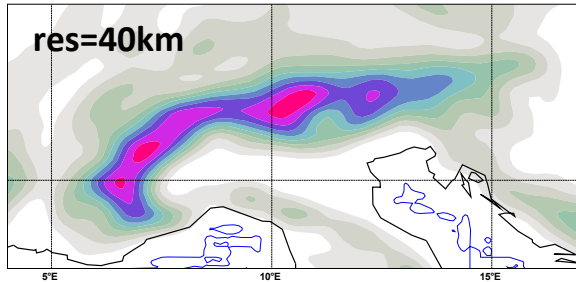
ERA40 standard deviation



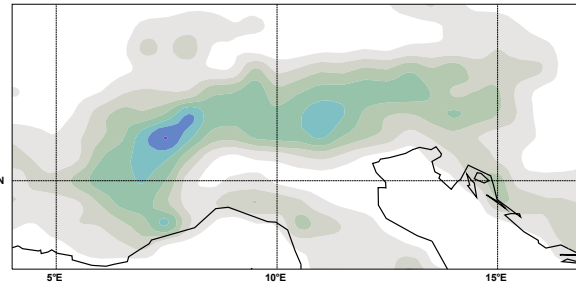
ERA40 slope



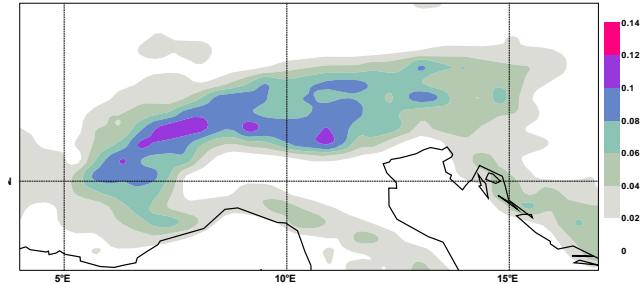
T511 mean orography/land sea mask



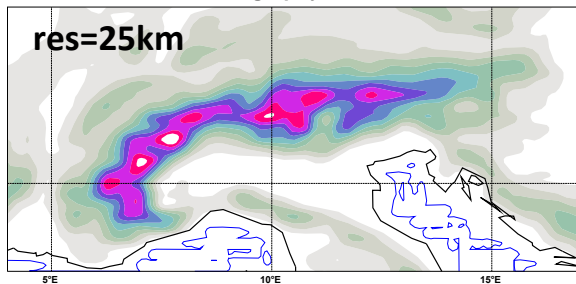
T511 standard deviation



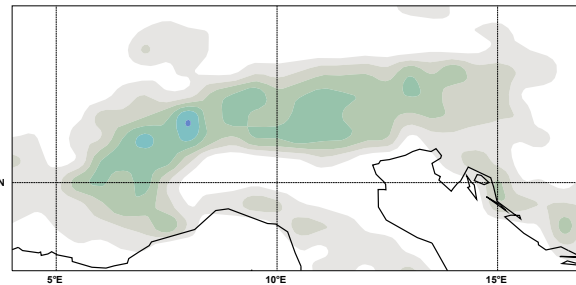
T511 slope



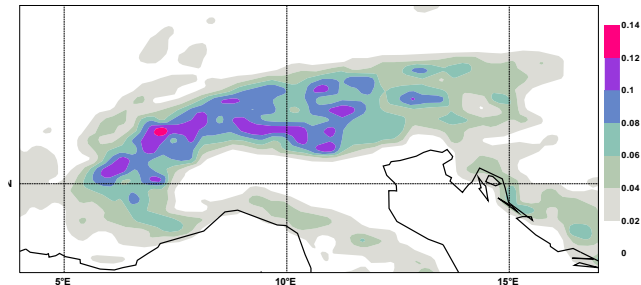
T799 mean orography/land sea mask



T799 standard deviation

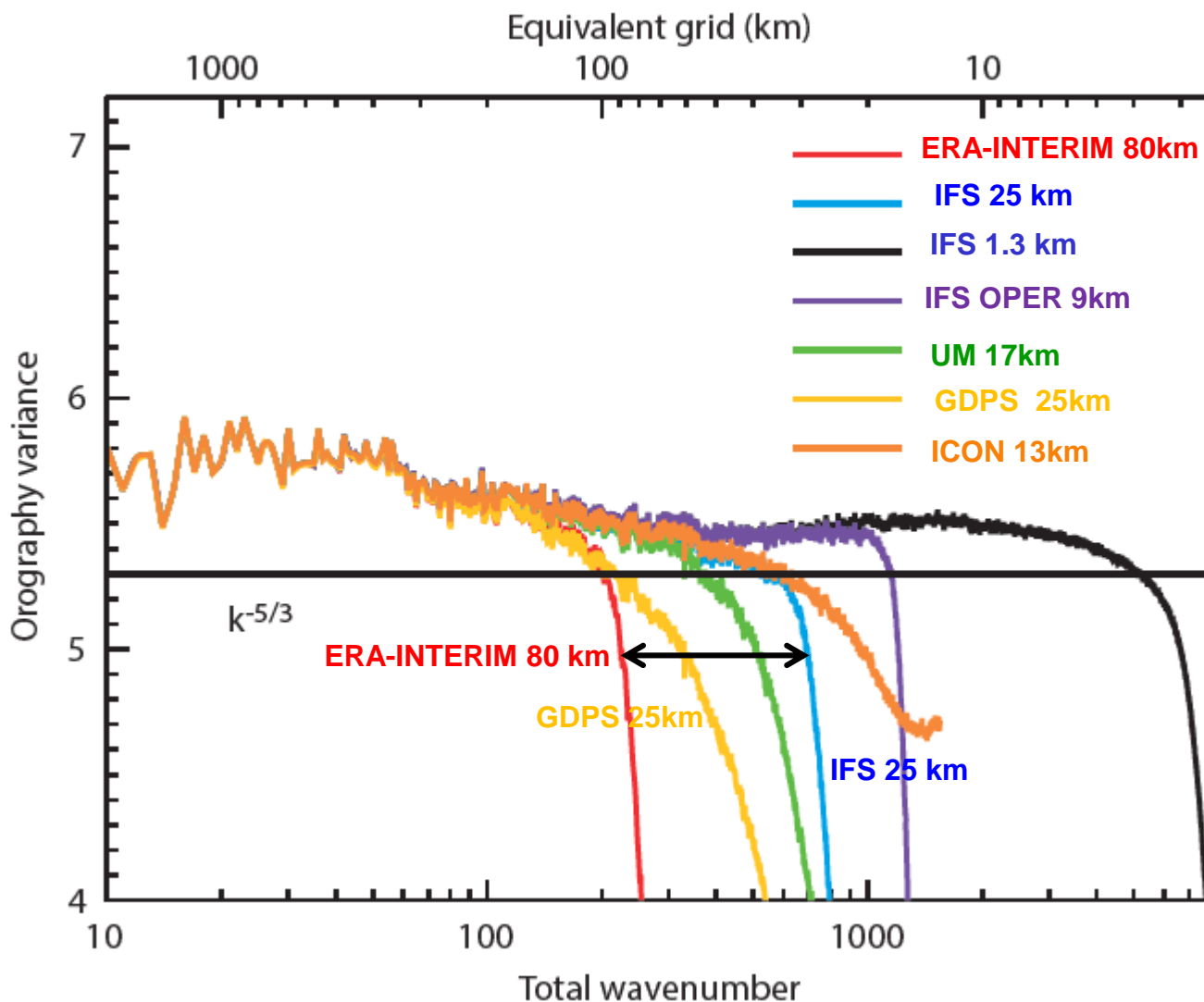


T799 slope



Horizontal resolutions: ERA40~120km; T511~40km; T799~25km

Differences in resolved orography



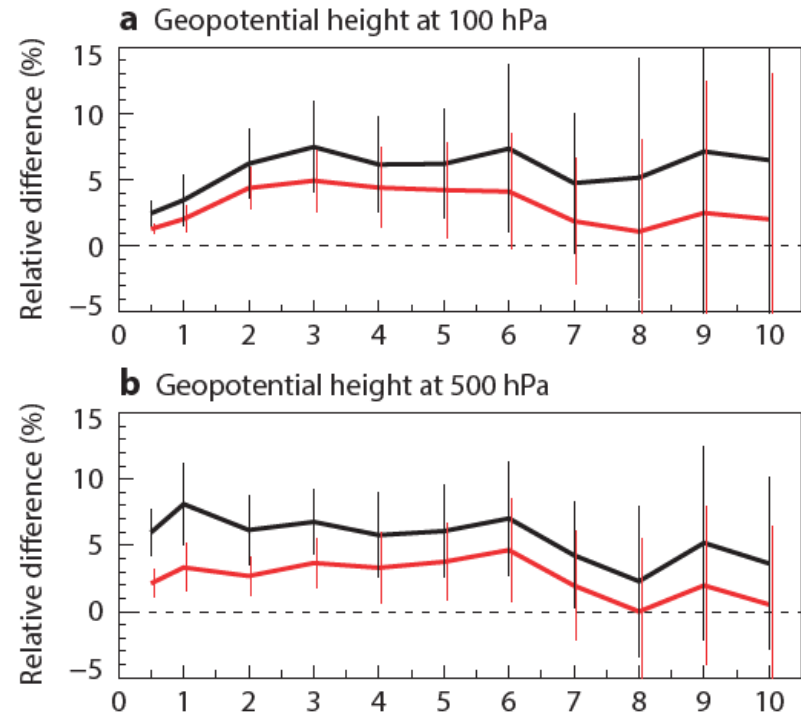
Impact of resolved orography on forecast skill

CTL – IFS 25km

EXP1: 25 km with 80km resolved orography

EXP2: 25 km with 80km resolved
and subgrid orography

Using a smoother resolved orography degrades significantly the forecast skill in terms of large-scale circulation, and near surface temperatures (during winter in the NH)



Consider stationary waves forced by sinusoidal orography with elevation $h(x)$: *two regimes*

$k > N/U$ (i.e. narrow-ridge case)

(or equivalently $U\pi/L > N$, i.e. high frequency)

Evanescent solution (i.e. fading away)

Non-dimensional length $NL/U < \pi$

- waves decay exponentially with height
- vertical phase lines
- linear theory -> no drag. Steep small scales leading to form drag -> TOFD scheme

$$w = Ae^{-|m|z} \cos kx$$

$k < N/U$ (i.e. wider mountains)

(or equivalently $U\pi/L < N$, i.e. low frequency)

Wave solution

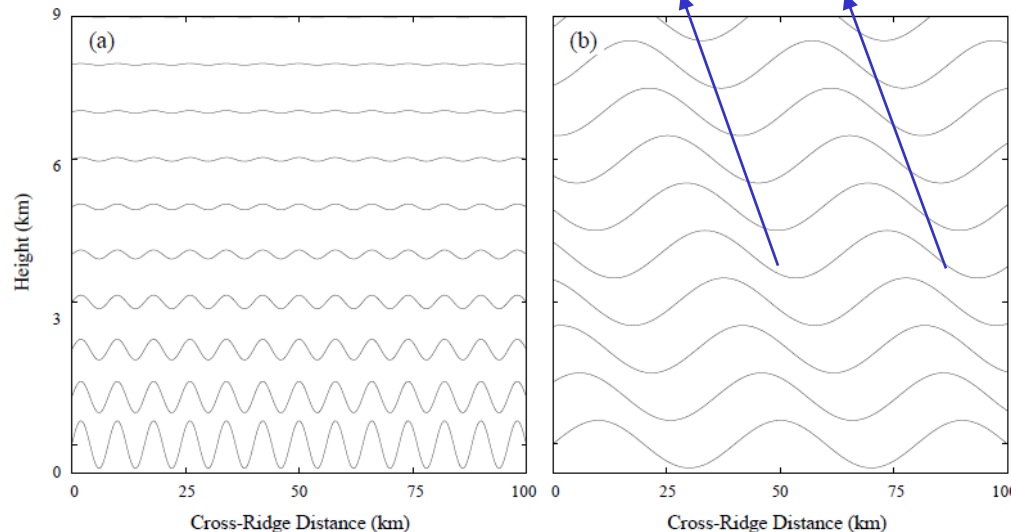
Non-dimensional length $NL/U > \pi$

- energy/momentum transported upwards
- waves propagate without loss of amplitude
- phase lines tilt upstream as z increases

$$w = A \cos(kx + mz)$$

For typical atmospheric wind and stability ($U=10$ m/s and $N=0.01$ s⁻¹): $L \approx 3$ km

$$N^2 = g \frac{d \ln \theta(z)}{dz}$$



Subgrid drag (stress) mechanisms in the ECMWF model

Scales smaller than 5 km

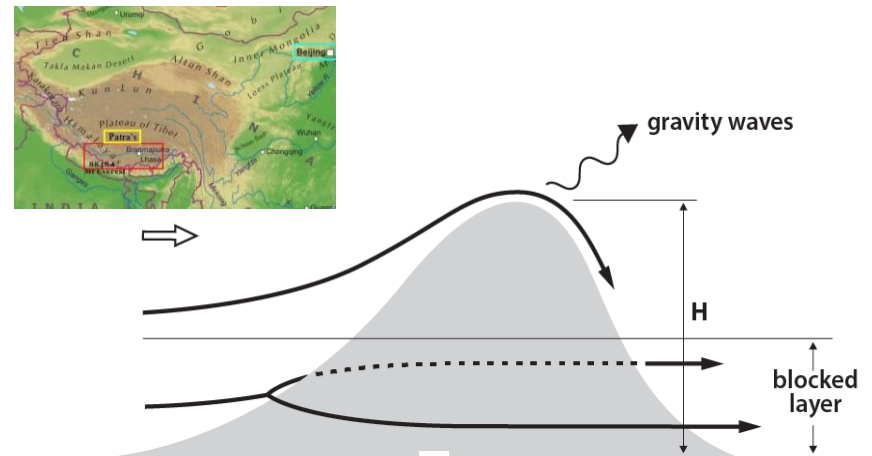


a) Turbulent Drag - TURB: Traditional MO transfer law with roughness for land use and vegetation

b) Turbulent Orographic Form Drag - TOFD: drag from small scale orography (Beljaars et al. 2004); Other models use orographic enhancement of roughness

waves are evanescent and flow around steep orographic features will lead to form drag

Scales larger than 5 km



a) Gravity Wave Drag - GWD: gravity waves are excited by the “effective” sub-grid mountain height, i.e. height where the flow has enough momentum to go over the mountain

b) Orographic low level blocking - BLOCK: strong drag at lower levels where the flow is forced around the mountain

Since 2006 ECMWF uses “Turbulent Orographic Form Drag (TOFD)” implemented as a tendency (or flux divergence) on model levels

Orographic form drag (simplified Wood and Mason, 1993):

$$\frac{\tau_{os}}{\rho} = 2\alpha\beta C_m \theta^2 U^2 (h_m)$$

α, β Shape parameters

C_m Drag coefficient

θ Silhouette slope

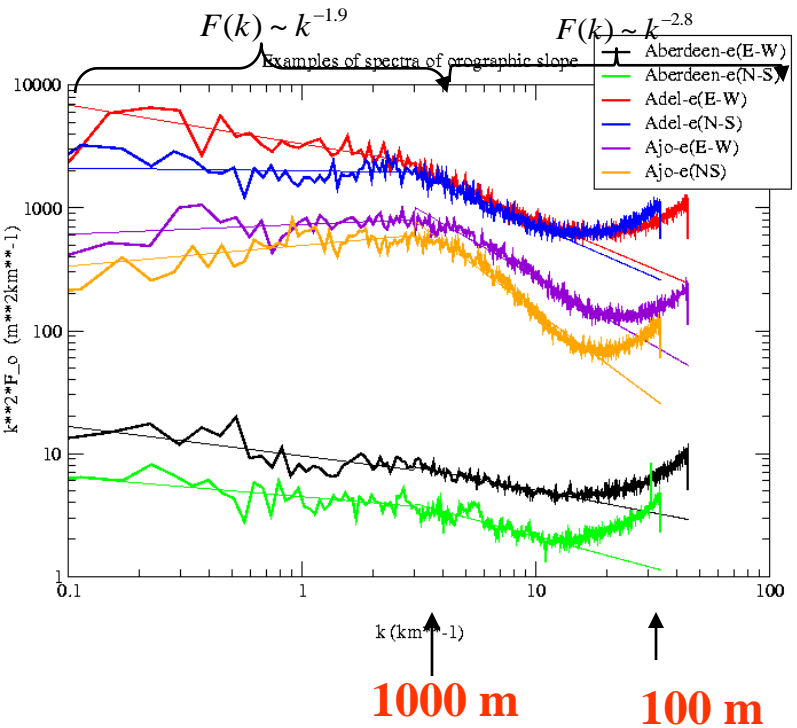
U Wind speed

h_m Reference height

Vertical distribution (Wood et al, 2001):

$$\tau_o = \tau_{os} e^{-z/h_m}$$

Parameterization of TOFD flux divergence with a continuous orographic spectrum:



$$\frac{\partial \tau_o}{\partial z} = \frac{-2\rho\alpha\beta C_m}{h_m} \theta^2 U^2(h_m) e^{-z/h_m}$$

Assume: $h_m \sim \min(2/k, 2/k_1)$ $k_1 = 0.003 \text{ m}^{-1}$

$$\theta^2 = \int_{k_o}^{\infty} k^2 F(k) dk$$

Write flux divergence as:

$$\frac{\partial \tau_o}{\partial z} = -2\rho\alpha\beta C_m \int_{k_o}^{\infty} \frac{k^2}{h_m} F(k) U^2(c_m / k) e^{-zk/c_m} dk$$

Beljaars, Brown and Wood, 2004, QJRMS, 130, 1327–1347



Subgrid drag (stress) mechanisms in the ECMWF model

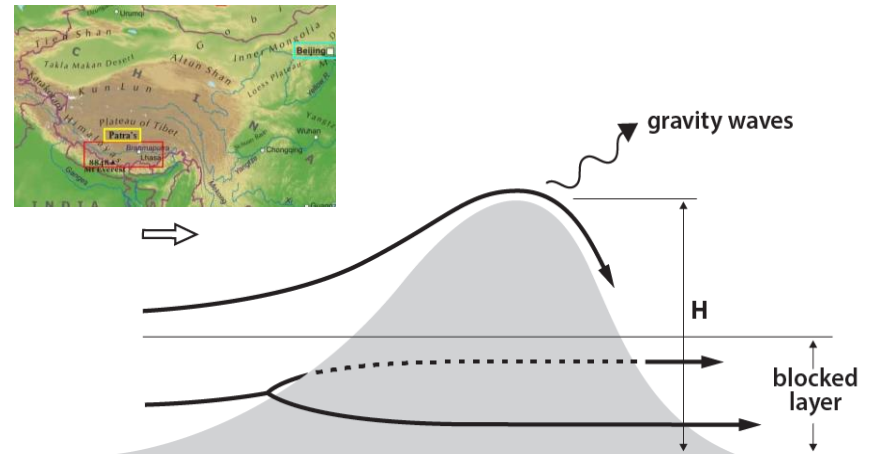
Scales smaller than 5 km



a) Turbulent Drag - TURB: Traditional MO transfer law with roughness for land use and vegetation

b) Turbulent Orographic Form Drag - TOFD: drag from small scale orography (Beljaars et al. 2004); Other models use orographic enhancement of roughness.

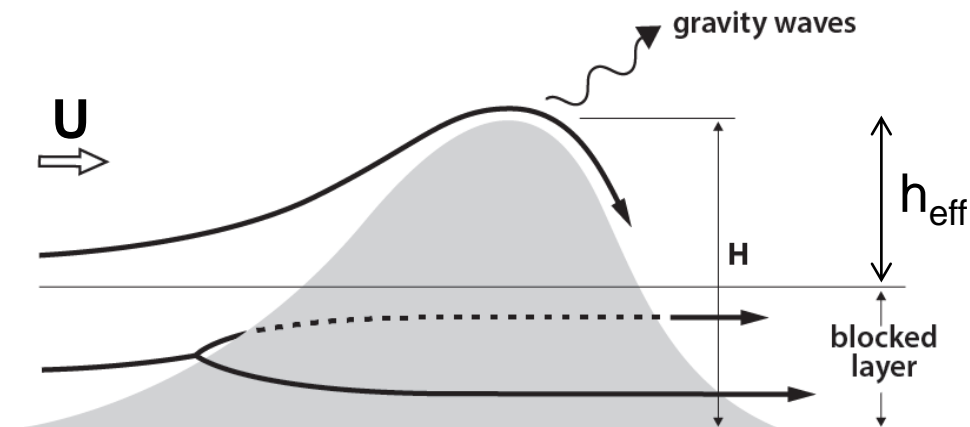
Scales larger than 5 km



a) Gravity Wave Drag - GWD: gravity waves are excited by the “effective” sub-grid mountain height, i.e. height where the flow has enough momentum to go over the mountain

b) Orographic low level blocking - BLOCK: strong drag at lower levels where the flow is forced around the mountain

Low-level blocking and gravity wave drag scheme (Lott and Miller 1997)



- linear/flow-over regime (NH/U small)
- non-linear/blocked regime (NH/U large)

Blocking occurs if surface air has less kinetic energy than the potential energy barrier presented by the mountain

$$h_{eff} = H_c U / N$$

$$z_{blk} = H - h_{eff}$$

Height h_{eff} is such that the Froude number Nh_{eff}/U reaches its critical value H_c

See Hunt and Snyder (1980)

The surface drag due to blocking and gravity wave generation

Drag at height z below blocking height applied on model levels:

$$D_{blk}(z) = \rho C_d \max\left(2 - \frac{1}{r}, 0\right) \frac{\sigma}{2\mu} \left(\frac{z_{blk} - z}{z + \mu}\right)^{1/2} (B \cos^2 \psi + C \sin^2 \psi) \frac{U |U|}{2}$$

$$\text{with } r = \frac{\cos^2 \psi + \gamma \sin^2 \psi}{y \cos^2 \psi + \sin^2 \psi}$$

Gravity wave stress above blocking height:

$$\tau_{gwd} = \rho_H U_H N_H h_{eff}^2 \frac{\sigma}{4\mu} G(B \cos^2 \psi_H + C \sin^2 \psi_H, (B - C) \sin \psi_H \cos \psi_H)$$

- B,C,G are constants
 - Index H indicates the characteristic height (2μ)
 - Ψ is computed from θ and wind direction
 - Density of ellipses per grid box is characterized by μ/σ
- μ : Standard deviation
 σ : Slope
 θ : Orientation
 γ : Anisotropy

Gravity wave dissipation

Strongest dissipation occurs in regions where the wave becomes unstable and breaks down into turbulence, referred to as wave breaking:

- Convective instability: where the amplitude of the wave becomes so large that it causes relatively cold air to rise over less dense, warm air

$$N_{\min}^2 = N^2 \left\{ 1 + \frac{N \delta h}{U} \right\}$$

δh : amplitude of wave

N : mean Brunt-Vaisala frequency

- Kelvin-Helmholtz instability also important: associated with shear zones. Amplitude of wave is reduced such that Ri_{\min} reaches critical value of 0.25 (saturation hypothesis; Lindzen 1981)

$$Ri_{\min} = \frac{N^2}{\eta^2} = Ri \left\{ \frac{1 - \alpha}{(1 + Ri^{1/2} \alpha^2)^2} \right\}$$

$$\alpha = N |\delta h| / U$$

$$\eta = \partial U / \partial z$$

δh : amplitude of wave

Ri : mean Richardson number

Subgrid orography scheme used as input for the Lott and Miller scheme

- Elliptically shaped mountains are assumed with aspect ratio a/b , and orientation ψ with respect to the wind
- Elliptic mountains are equally spaced
- Subgrid orography is characterized by:
 - Standard deviation μ
 - Slope σ
 - Orientation θ
 - Anisotropy γ (1:circular; 0: ridge)

$$\gamma^2 = \frac{K - (L^2 + M^2)^{1/2}}{K + (L^2 + M^2)^{1/2}}$$

$$\theta = 0.5 \tan^{-1}(M / L)$$

$$\sigma^2 = K + (L^2 + M^2)^{1/2}$$

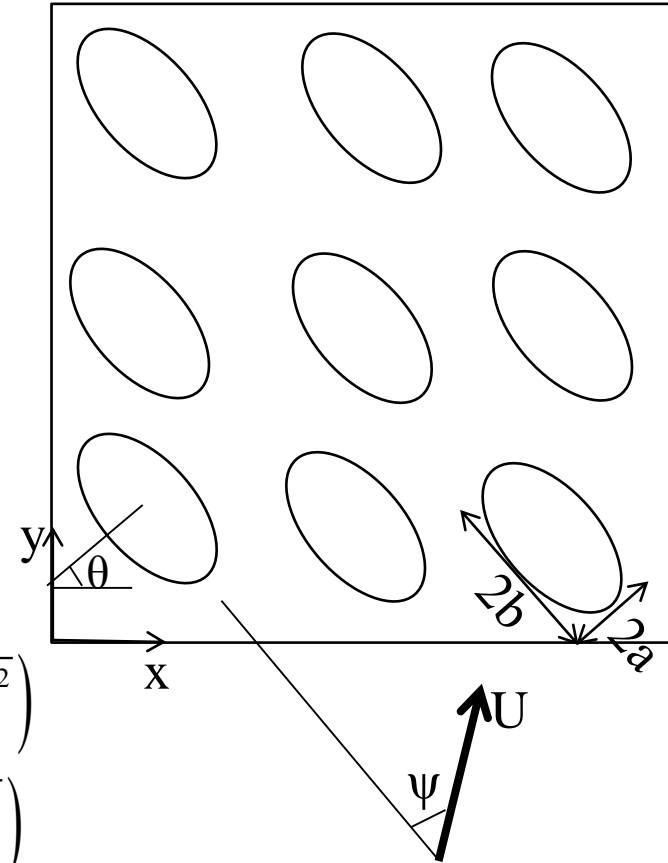
$$\mu^2 = \overline{h^2} - (\overline{h})^2$$

$$K = 0.5 \left(\overline{(\partial h / \partial x)^2} + \overline{(\partial h / \partial y)^2} \right)$$

$$L = 0.5 \left(\overline{(\partial h / \partial x)^2} - \overline{(\partial h / \partial y)^2} \right)$$

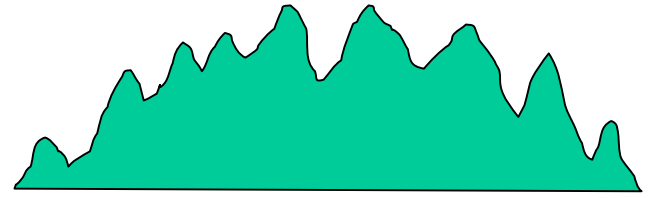
$$M = \overline{(\partial h / \partial x)(\partial h / \partial y)}$$

Conceptual picture of model grid box



Preparation of the data sets to characterize the sub-grid orography

1. Global 1km resolution surface elevation data

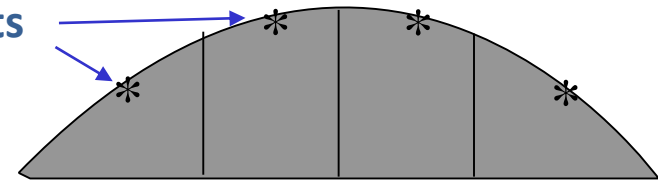


2. Reduce to 5 km resolution by smoothing



3. Compute mean orography at model resolution

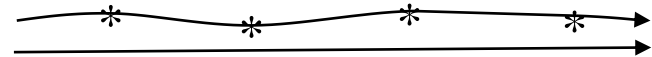
gridpoints



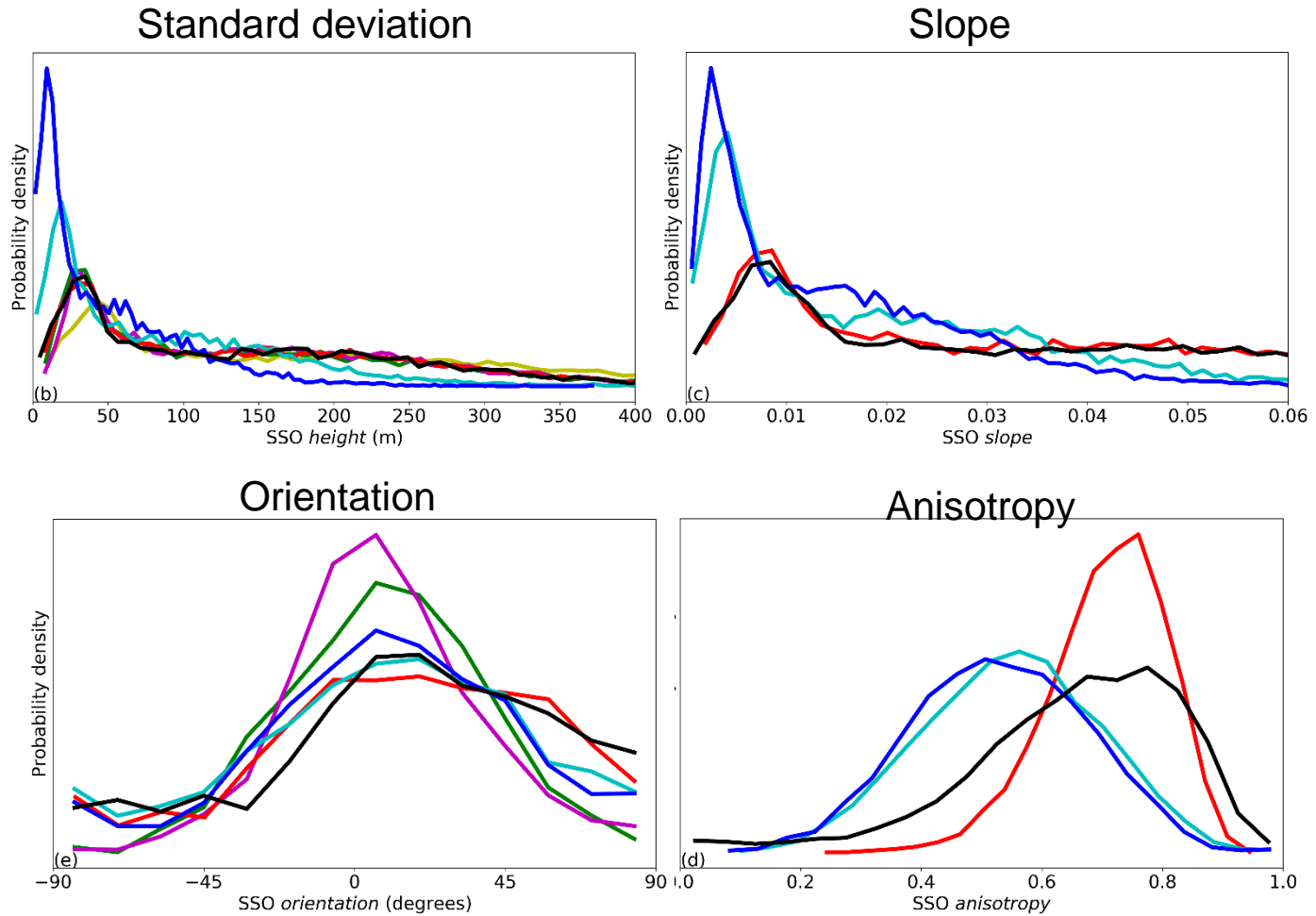
4. Subtract model orography (3) from 5km orography (2)



5. Compute standard deviation, slope, orientation and anisotropy for every grid box



Large inter-model spread in subgrid orography fields in NWP models



Numerics of fast processes

The time scales of flow blocking, TOFD and turbulent diffusion are short at the lowest model levels and raise stability issues. The tendency from these processes can be written as :

$$\frac{dU}{dt} = D - C|U|U$$

$$\frac{dV}{dt} = D - C|U|V \quad \text{where} \quad C = C_{vdf} + C_{block} + C_{tofd}$$

To minimize time step dependencies, the three schemes are solved for together in one implicit computation:

$$\frac{U^{n+1} - U^n}{\Delta t} = D^n - C^n |U^n| \{ \alpha U^{n+1} + (1 - \alpha) U^n \}$$

$$\frac{V^{n+1} - V^n}{\Delta t} = D^n - C^n |U^n| \{ \alpha V^{n+1} + (1 - \alpha) V^n \}$$

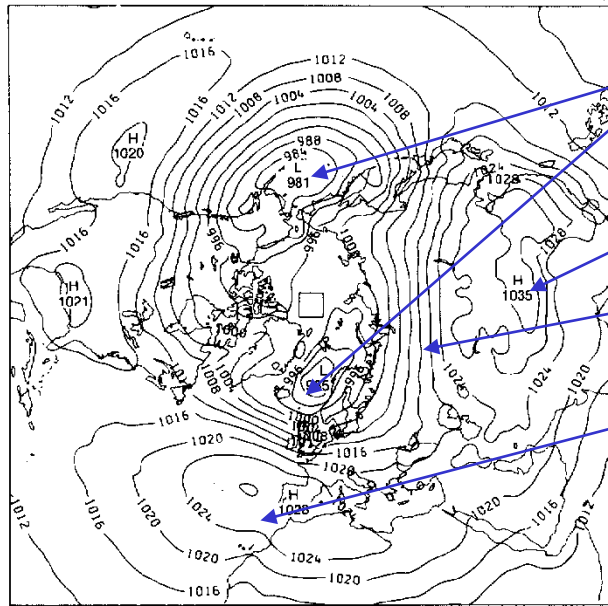
$\alpha = 1.5$ to avoid (non-linear) instabilities in the vertical diffusion scheme.

See: Orr (2007), Evaluation of revised parametrizations of sub-grid orographic drag, ECMWF Technical Memorandum 536.

Impact of the Lott and Miller scheme

Alleviation of systematic westerly bias in low resolution model (2.5°x3.75°) in 1985

CONTROL EXPERIMENT (C)



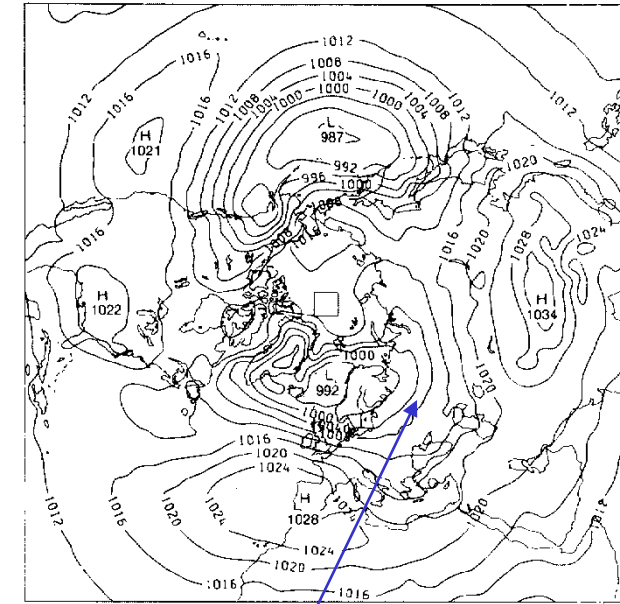
Icelandic/Aleutian lows are too deep

Siberian high too weak and too far south

Flow too zonal / westerly bias

Azores anticyclone too far east

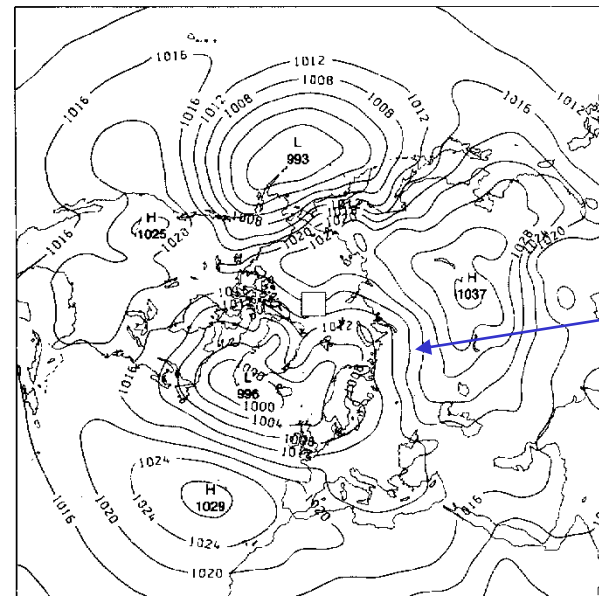
GRAVITY WAVE EXPERIMENT (G)



With GWD scheme
alleviation of westerly bias

Without GWD scheme

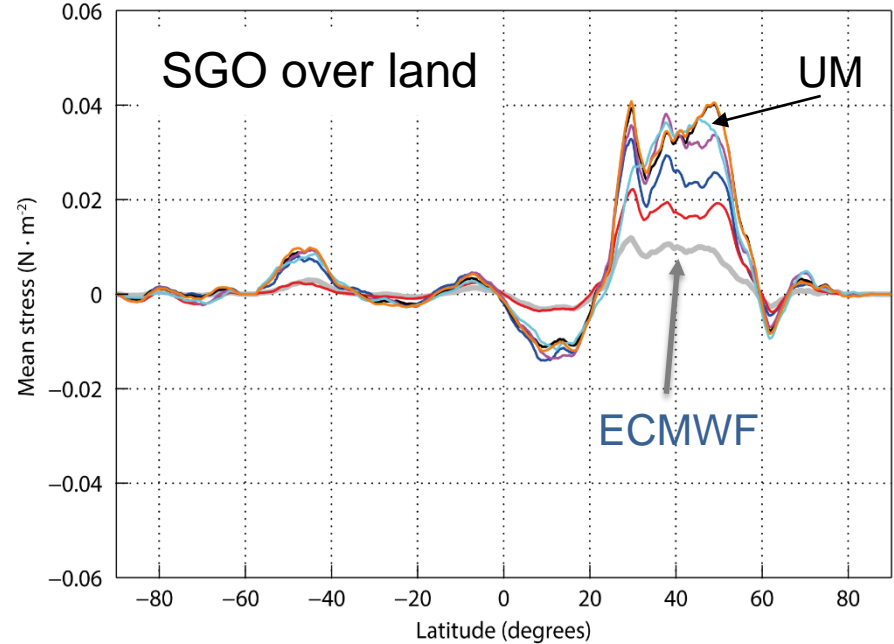
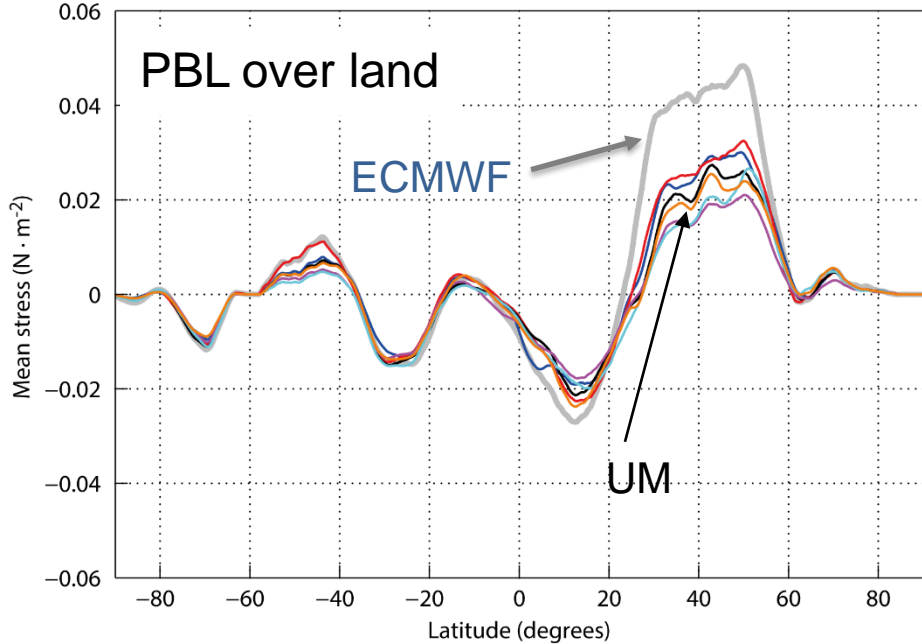
MEAN JANUARY 1984-1986



Analysis (best guess)

better agreement

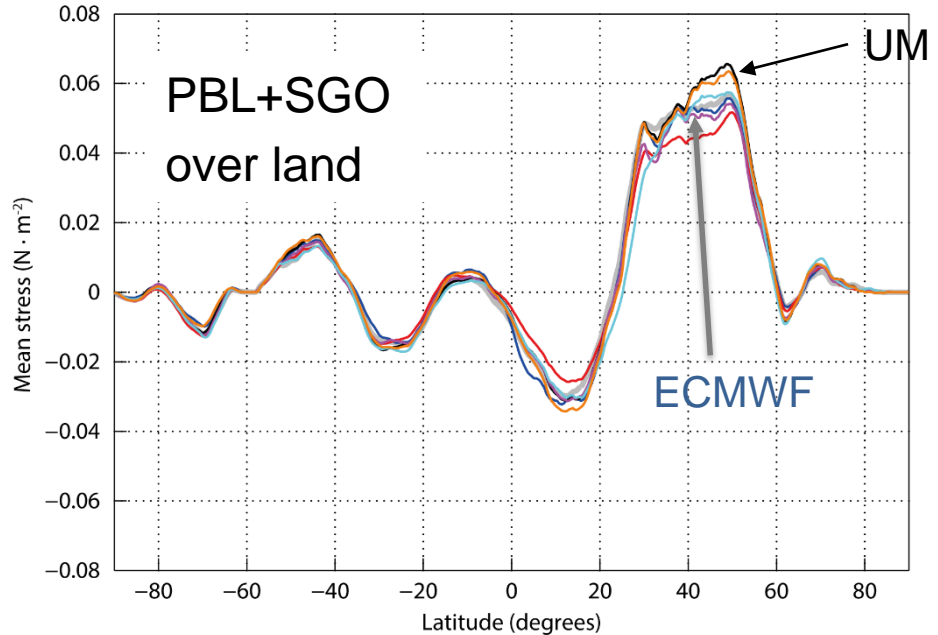
From Palmer et al. 1986



— IFS (ECMWF) — GM (UKMetO) — GSM (JMA) — ACCES (ABOM)
 — GDPS (CMC) — ICON (DWD) — ARPEGE (MeteoFrance)

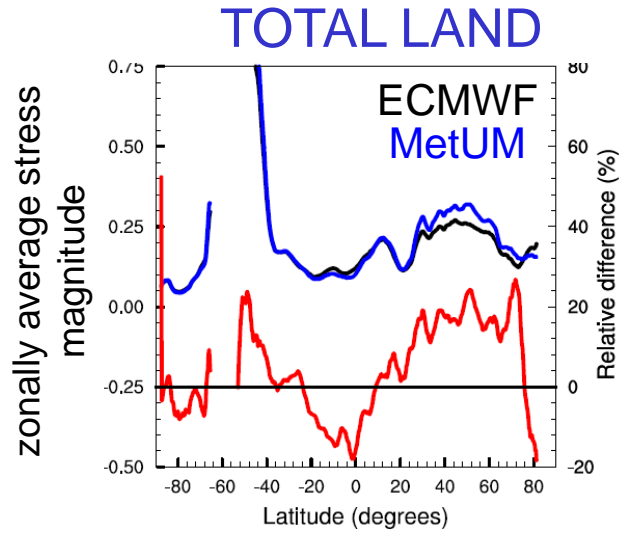
— IFS (ECMWF) — GM (UKMetO) — GSM (JMA) — ACCES (ABOM)
 — GDPS (CMC) — ICON (DWD) — ARPEGE (MeteoFrance)

WGNE Drag project
 – comparison of
 surface stress

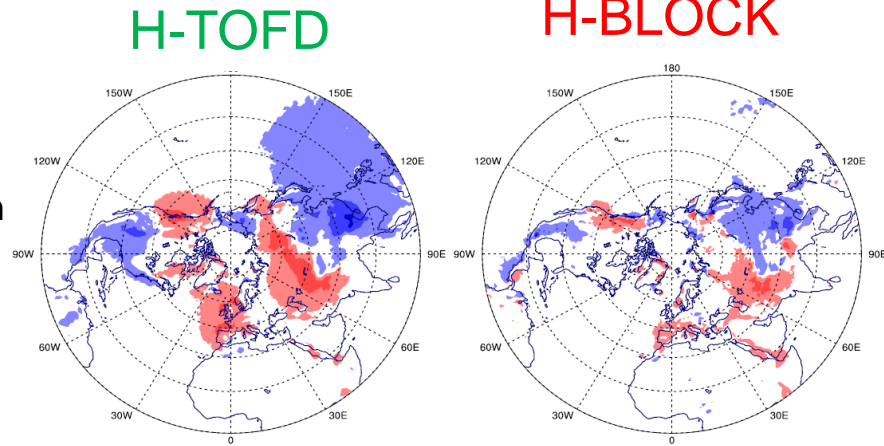


— IFS (ECMWF) — GM (UKMetO) — GSM (JMA) — ACCES (ABOM)
 — GDPS (CMC) — ICON (DWD) — ARPEGE (MeteoFrance)

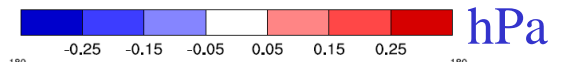
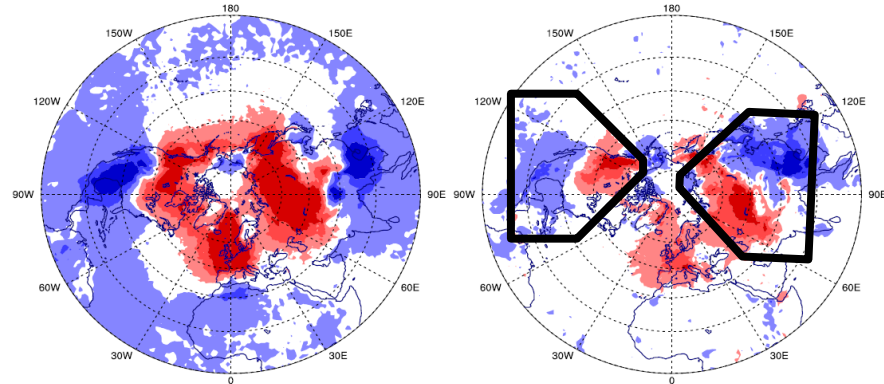
Inter-model differences in orographic drag (and its partition) impact circulation



Mean change in
SP +6h

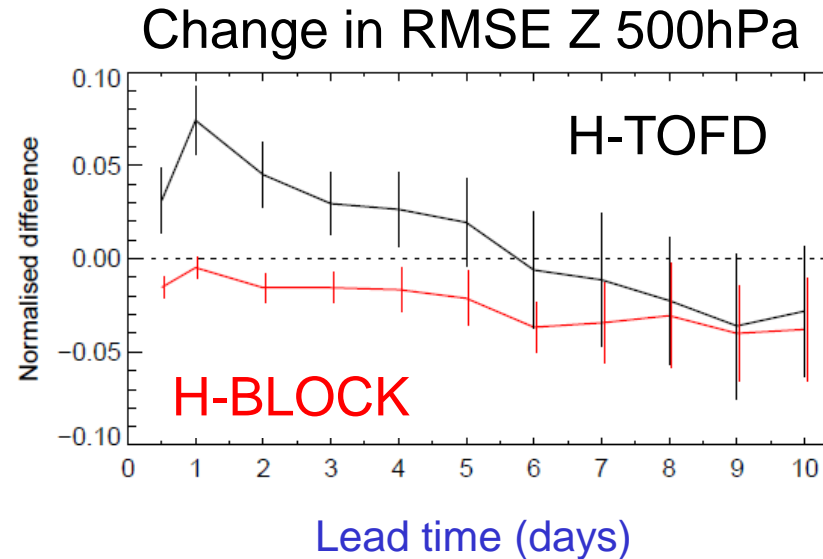


Mean change in
SP +24h



Sandu et al. 2016, JAMES

Inter-model differences in orographic drag (and its partition) impact circulation



Fine balance between improving and degrading the forecast!

It matters how the drag is partitioned between the two schemes

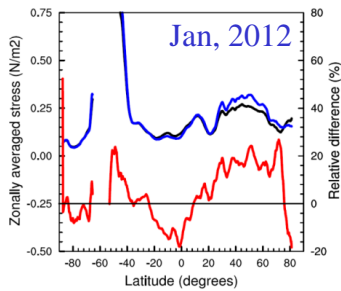
Quasi-identical response for H-TOFD at 16km

The trouble won't go away with high resolution anytime soon!

Changes in surface stress also affect longer timescales (seasonal to climate)
See Sigmond and Scinocca, 2010, Sandu et al. 2016, Pithan et al., 2015,2016,
Van Niekerk et al 2017

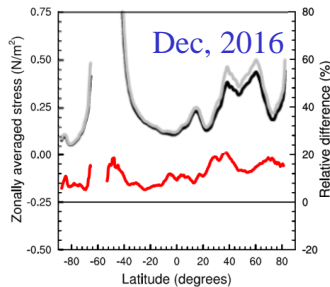
How much do the subgrid orography fields contribute to inter-model spread in surface stress?

IFS experiments where SSO fields are substituted with MetUM SSO fields



Zadra (2013)

IFS
MetUM
Relative diff.

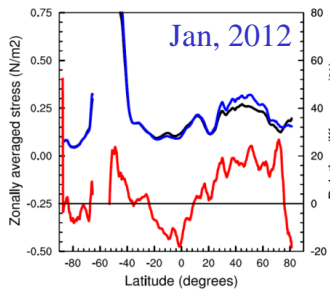


IFS
IFS with MetUM
SSO fields
Relative diff.

Inter-model variability in SSO fields can be of first-order importance to the variability in surface stress seen across models

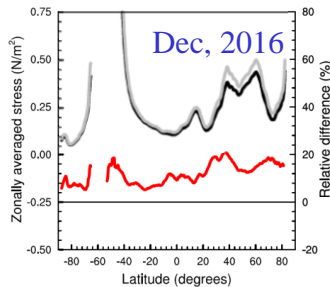
How much do the subgrid orography fields contribute to inter-model spread in surface stress?

IFS experiments where SSO fields are substituted with MetUM SSO fields



Zadra (2013)

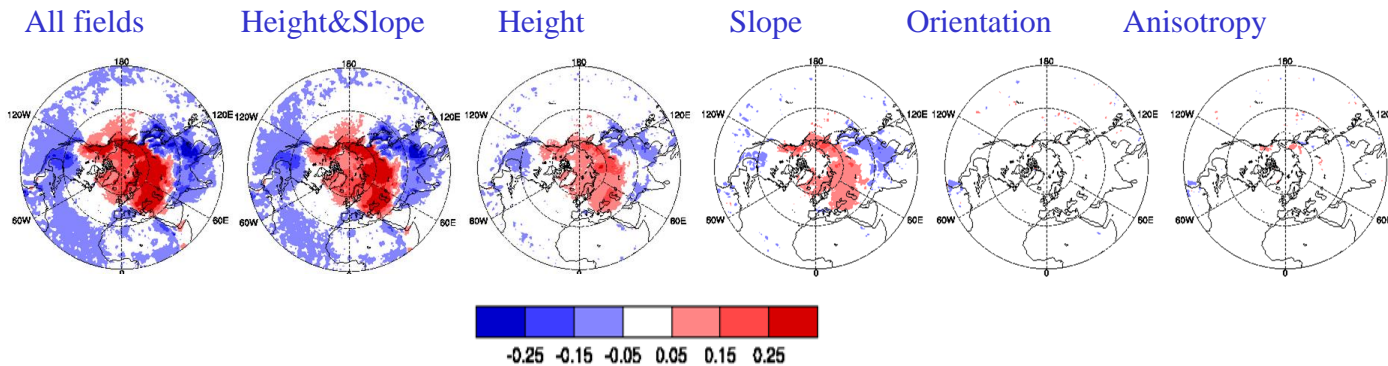
IFS
MetUM
Relative diff.



IFS
IFS with MetUM
SSO fields
Relative diff.

Inter-model variability in SSO fields can be of first-order importance to the variability in surface stress seen across models

Combined effect of *height* & *slope* required to explain response in surface pressure (t+24h)



In summary:

Models don't agree:

- in the resolved orography, nor in the subgrid orography
- in total subgrid drag, nor in its partition between different processes and the diurnal cycle, particularly over orography
- The differences in subgrid drag and in its partition are partly the result of repeated tuning exercises designed to improve model skill (NWP or climate), also strongly related to the derivation of the subgrid orography fields

Subgrid orographic drag processes:

- have a large impact on the large-scale circulation, at all timescales
- are responsible for known systematic circulation biases
- the orographic drag parametrizations are fairly simplistic and especially poorly constrained, and don't necessarily behave well with resolution (van Niekerk, 2016, Vosper, 2016)

The way forward: constraining drag processes

Use observations, inverse modelling and high resolution simulations to better understand these processes, identify caveats of existing parameterizations, and improve upon them, and thereby reduce the associated systematic errors

Sandu et al., perspective, NPJ Climate and atmospheric science, 2019

COncstraining ORographic Drag Effects (**COORDE**)

Annelize van Niekerk (Met Office) & Irina Sandu (ECMWF)

A GASS/WGNE intercomparison

Understanding the effects of resolved and parametrized orographic drag through the **COORDE**-nation of different modeling groups.

Aims:

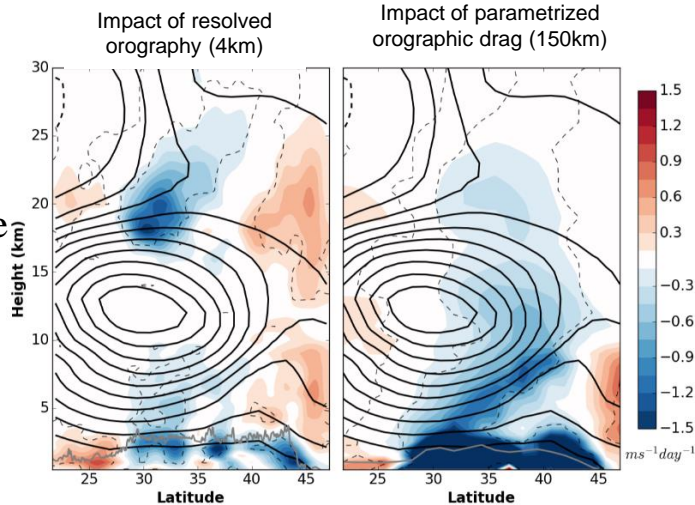
- Expose differences in orographic drag parametrization formulation between models
- Understand impacts of differences in orographic drag parametrizations for modelled circulation
- Use high resolution simulations to quantify drag from small-scale orography, typically unresolved in models used for climate/seasonal projections, in order to evaluate orographic drag parametrizations
- Understand differences in resolved and parametrized orographic drag across models

Protocol: <https://osf.io/37bsyl/>

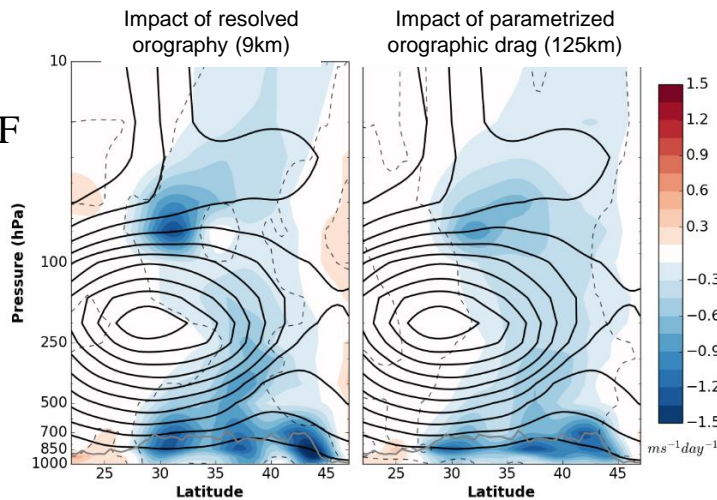
Participants currently include: Environment Canada, DWD, CMA, JMA, NOAA/NCEP, KIAPS, Meteo-France, Met Office and ECMWF.

COORDE

Met Office
UM

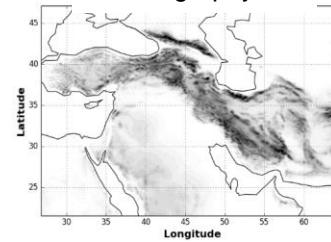


ECMWF
IFS

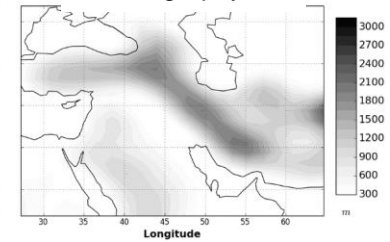


van Niekerk et al. (2018), JAMES

High resolution
orography



Low resolution
orography



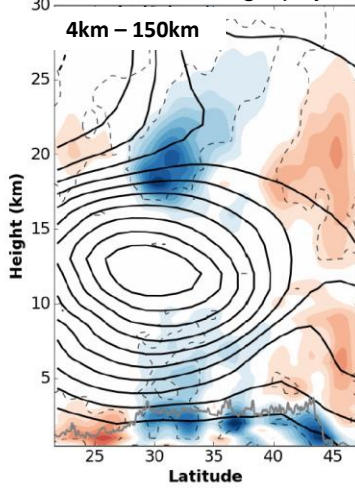
Method:

- 1) High resolution experiments (4km / 9km) with high resolution and low resolution orography are used to determine impact of resolved orography on circulation
- 2) Low resolution experiments (150km / 125km) with and without parametrized orographic drag used to determine impact of parametrized orographic drag on circulation

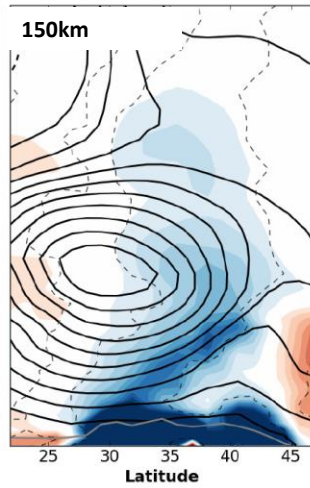
Plots show the impact of small-scale resolved orography (left) and parametrized orographic drag (right) on zonal winds in two models.

Middle East

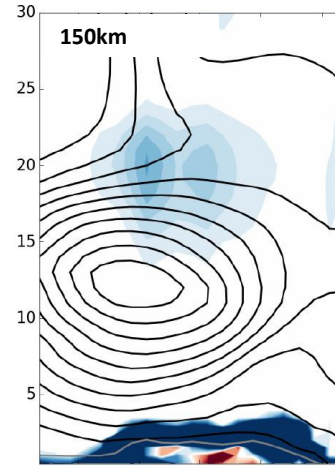
Impact of resolved orography



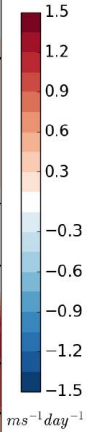
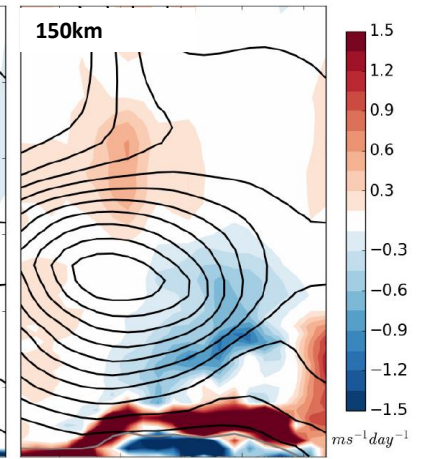
Impact of parametrized drag



SSO tendencies

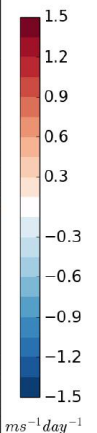
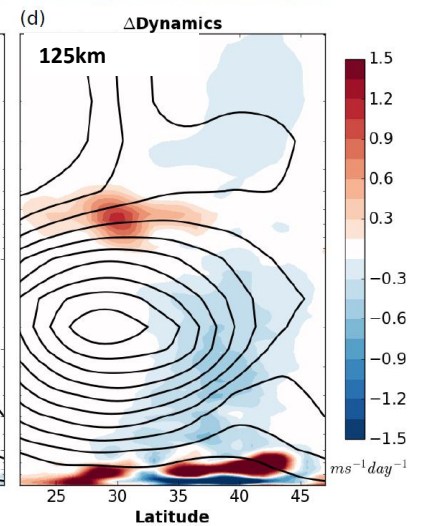
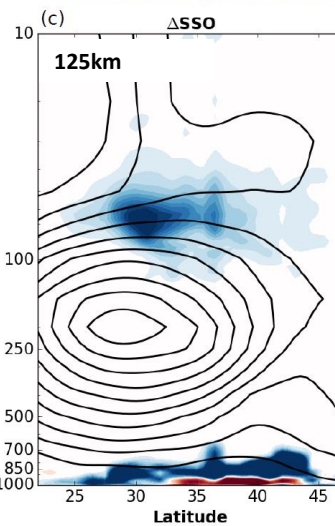
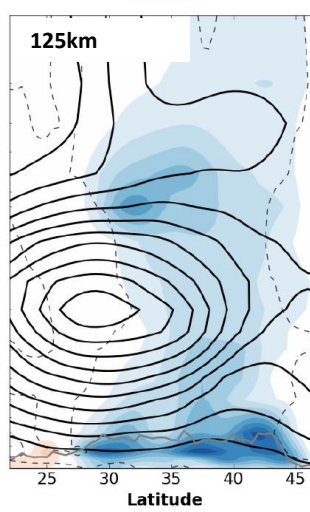
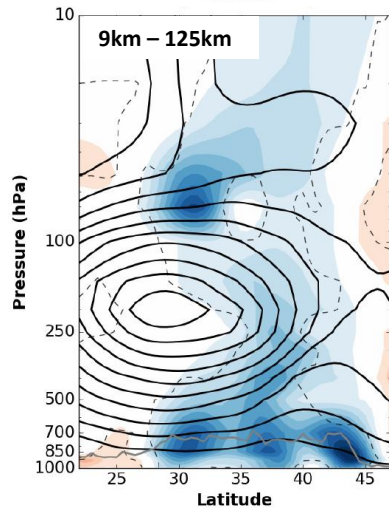


Dyn tendencies



MetUM

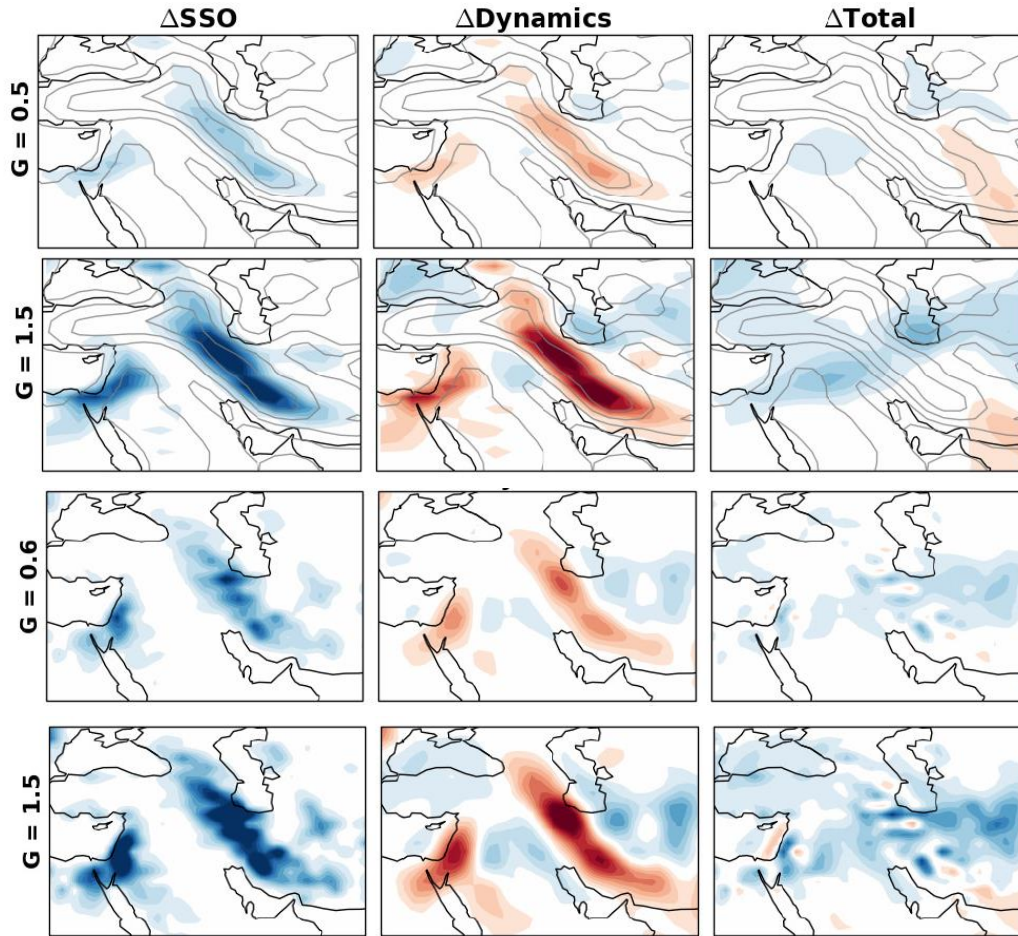
IFS



van Niekerk et al. (2018), JAMES

Middle East

MetUM



Errors in the circulation response induced by orographic drag at low/intermediate resolution are due to both the parametrizations and their coupling with the dynamics

IFS

van Niekerk et al. (2018), JAMES